

manuscript No. (will be inserted by the editor)

Shinya Aoi · Takahiro Kondo · Naohiro Hayashi ·
Dai Yanagihara · Sho Aoki · Hiroshi Yamaura ·
Naomichi Ogihara · Tetsuro Funato · Nozomi
Tomita · Kei Senda · Kazuo Tsuchiya

Contributions of phase resetting and interlimb coordination to the adaptive control of hindlimb obstacle avoidance during locomotion in rats: a simulation study

the date of receipt and acceptance should be inserted later

S. Aoi, T. Kondo, N. Hayashi, and K. Senda
Dept. of Aeronautics and Astronautics, Graduate School of Engineering, Kyoto University, Yoshida-honmachi,
Sakyo-ku, Kyoto 606-8501, Japan
Tel: +81-75-753-5809
Fax: +81-75-753-5809
E-mail: shinya_aoi@kuaero.kyoto-u.ac.jp

D. Yanagihara, S. Aoki, and H. Yamaura
Dept. of Life Sciences, Graduate School of Arts and Sciences, The University of Tokyo, 3-8-1 Komaba, Meguro-
ku, Tokyo 153-8902, Japan

N. Ogihara
Dept. of Mechanical Engineering, Faculty of Science and Technology, Keio University, 3-14-1 Hiyoshi, Kohoku-
ku, Yokohama 223-8522, Japan

T. Funato
Dept. of Mechanical Engineering and Science, Graduate School of Engineering, Kyoto University, Yoshida-
honmachi, Sakyo-ku, Kyoto 606-8501, Japan

N. Tomita and K. Tsuchiya
Dept. of Energy and Mechanical Engineering, Faculty of Science and Engineering, Doshisha University, 1-3
Tatara, Miyakodani, Kyotanabe, Kyoto 610-0394, Japan

S. Aoi, D. Yanagihara, N. Ogihara, N. Tomita, and K. Tsuchiya
JST, CREST, 5 Sanbancho, Chiyoda-ku, Tokyo 102-0075, Japan

Abstract Obstacle avoidance during locomotion is essential for safe, smooth locomotion. Physiological studies regarding muscle synergy have shown that the combination of a small number of basic patterns produces the large part of muscle activities during locomotion and the addition of another pattern explains muscle activities for obstacle avoidance. Furthermore, central pattern generators in the spinal cord are thought to manage the timing to produce such basic patterns. In the present study, we investigated sensory-motor coordination for obstacle avoidance by the hindlimbs of the rat using a neuromusculoskeletal model. We constructed the musculoskeletal part of the model based on empirical anatomical data of the rat and the nervous system model based on the aforementioned physiological findings of central pattern generators and muscle synergy. To verify the dynamic simulation by the constructed model, we compared the simulation results with kinematic and electromyographic data measured during actual locomotion in rats. In addition, we incorporated sensory regulation models based on physiological evidence of phase resetting and interlimb coordination, and examined their functional roles in stepping over an obstacle during locomotion. Our results show that the phase regulation based on interlimb coordination contributes to stepping over a higher obstacle and that based on phase resetting contributes to quick recovery after stepping over the obstacle. These results suggest the importance of sensory regulation in generating successful obstacle avoidance during locomotion.

Keywords Rat, locomotion, obstacle avoidance, neuromusculoskeletal model, central pattern generator, muscle synergy, phase resetting, interlimb coordination

1 Introduction

Humans and animals achieve adaptability of locomotion in diverse environments by cooperatively and skillfully controlling their complicated and redundant musculoskeletal systems. In the actual travel path, obstacles are often encountered that must be stepped over to continue locomotion. Stepping over obstacles to avoid tripping is an essential movement for safe, smooth locomotion. Such obstacle avoidance is a skillful, intentional movement, whereby humans and animals must recognize the dimensions of an obstacle, and determine how to control their limbs to avoid colliding with it while maintaining their posture. This task requires highly coordinated control of spatiotemporal patterns of command signals.

To date, the abilities of humans and animals to generate adaptive movements have been investigated by examining the configurations and activities of neural systems. For example, physiological studies with lampreys and cats have greatly contributed to elucidating locomotor mechanisms (Grillner 1975; Orlovsky *et al.* 1999; Shik and Orlovsky 1976; Yanagihara *et al.* 1993; Yanagihara and Kondo 1996). However, locomotion is a well-organized motion generated by dynamic interactions among the body, the nervous system, and the environment. It is difficult to fully analyze locomotion mechanisms solely in terms of the nervous system. As well as understanding the nervous system, it is crucial to elucidate dynamic characteristics inherent in the body. Integrative studies of the musculoskeletal and nervous systems are required to clarify locomotion mechanisms.

Anatomical and physiological findings now enable the construction of reasonably realistic models of the musculoskeletal and nervous systems. Thus, to overcome the limitations of behavioral studies based only on the nervous system, simulation studies have recently investigated specific functional roles of the nervous system in locomotor behavior (Aoi *et al.* 2010; Aoi *et al.* 2012; Ekeberg and Pearson 2005; Ivashko *et al.* 2003; Jo and Massaquoi 2007; Jo 2008; Markin *et al.* 2010; Taga *et al.* 1991; Taga 1995; Taga 1998; Yakovenko *et al.* 2004).

Physiological studies have shown the importance of the concepts of the central pattern generator (CPG) (Grillner 1975; Orlovsky *et al.* 1999; Shik and Orlovsky 1976) and muscle synergy (d'Avella and Bizzi 2005; d'Avella *et al.* 2003; Drew *et al.* 2008; Ivanenko *et al.* 2005; Latash 2008; Ting and Macpherson 2005; Todorov and Jordan 2002). In particular, although the electromyographic (EMG) data recorded during locomotion are complex, they can be accounted for by the combination of only a small number of basic patterns (d'Avella and Bizzi 2005; d'Avella *et al.* 2003; Dominici *et al.* 2011; Ivanenko *et al.* 2004; Ivanenko *et al.* 2005; Ivanenko *et al.* 2006). Furthermore, CPGs are thought to manage the timing necessary to produce such basic patterns during locomotion (Ivanenko *et al.* 2006). In our previous work (Aoi *et al.* 2010), we developed a neuromusculoskeletal model of human walking based on

these physiological findings while incorporating a sensory regulation model based on the physiological evidence of phase resetting (Lafreniere-Roula and McCrea 2005; Duysens 1977; Rybak *et al.* 2006a; Schomburg *et al.* 1998) and investigated the sensory-motor coordination for generating adaptive locomotor behavior.

Because rodents are often used as experimental animals to examine the roles of the nervous system in generating various movements (Akay *et al.* 2006; Gruner *et al.* 1980; Ichise *et al.* 2000; Pearson *et al.* 2005; Sato *et al.* 2012), to further examine the contributions of CPGs and muscle synergy, in the present study we investigated rats stepping over an obstacle during locomotion over a flat surface, by constructing a similar neuromusculoskeletal model. Analysis of muscle synergy has also shown that the addition of another pattern to the basic patterns of locomotion explains the muscle activities for obstacle avoidance (Ivanenko *et al.* 2005; Ivanenko *et al.* 2005). This means that the additional pattern controls the intralimb (intersegmental) coordination of limb movements to enable obstacle avoidance. We modified our nervous system model (Aoi *et al.* 2010) for rat locomotion and incorporated this physiological finding for obstacle avoidance into the new nervous system model. We also developed a musculoskeletal model of the hindlimbs of the rat based on empirical anatomical data and constructed a neuromusculoskeletal model by integrating the musculoskeletal and nervous system models. To determine the validity of the dynamic simulation produced by this integrated model, we then compared the simulation results with measured kinematic and EMG data during rat locomotion. We incorporated sensory regulation models based on phase resetting and interlimb coordination to examine the contribution of the sensory-motor integration to the adaptive control of stepping over an obstacle during locomotion.

2 Empirical experiments with rats

We used five adult male Wistar rats (125 ± 10 g body weight) to construct the musculoskeletal model of the hindlimbs of the rat and to collect EMG data during locomotion (Kondo *et al.* 2010): one to verify the musculoskeletal model by electrical stimulation of muscles and four to collect the EMG data during locomotion (see Section 2.2). After recording locomotor data, the rats were deeply anesthetized and musculoskeletal features were measured (see Section 2.1). In addition, to obtain the kinematics of hindlimbs during locomotion and stepping over obstacles, we used an additional adult male Wistar rat (270 g body weight) (Sato *et al.* 2012) (see Section 2.2). Although the rats used to generate the anatomical and EMG data were smaller than that used to obtain the hindlimb kinematics, the relative measurements, such as length and mass, and EMG data were consistent with those of previous studies (Akay *et al.* 2006; Gruner *et al.* 1980; Johnson *et al.* 2008; Pearson *et al.* 2005). The rats were maintained under a 12 : 12 hour light-dark cycle before the day of the experiment. The experiments were approved by the Ethical Committee for Animal Experiments at the University of Tokyo, and were carried out in accordance with the Guidelines for Research with Experimental Animals of the University of Tokyo and the Guide for the Care and Use of Laboratory Animals (NIH Guide) revised in 1996. All efforts were made to minimize the number of animals used and their suffering throughout the course of the experiments.

2.1 Anatomical data for the musculoskeletal model

For the skeletal model, we measured physical parameters of the rats, such as masses, joint positions, and distances between joints, and determined the model parameters from these measurements (see Section 3.1). For the muscle model, we focused on seven principal muscles for the hindlimbs; five uniarticular: hip flexion (iliopsoas, IP), hip extension (gluteus maximus, GM), knee extension (vastus lateralis, VL), ankle flexion (tibialis anterior, TA), and ankle extension (soleus, SO), and two biarticular: hip extension and knee flexion (biceps femoris, BF), and knee flexion and ankle extension (gastrocnemius, GA). We first electrically stimulated individual muscles and determined which joint moves were needed to verify our musculoskeletal model. For example, we confirmed whether the hip joint extends and the knee joint flexes when we electrically stimulate the BF muscle. We measured the attachment, direction, and physiological cross-sectional area (PCSA) for each muscle and determined the model parameters from these measurements (see Section 3.1).

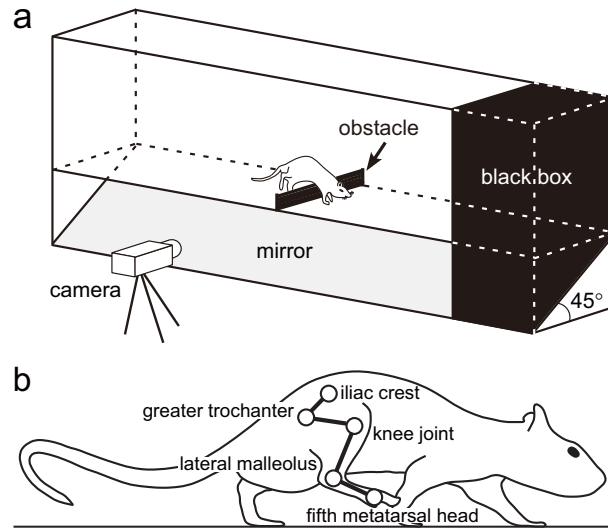


Fig. 1 Experimental setup (a) and rat with markers (b) for measuring locomotion in rats. a is modified from (Sato *et al.* 2012).

2.2 Kinematic and EMG data

Two weeks before the recording of locomotion, the rats were habituated to the custom-made runway apparatus (length: 140 cm, width: 14 cm) constructed from transparent acrylic board (thickness: 3 mm) (Fig. 1a). The obstacle was attached at the midpoint of the runway. Reflected images in a mirror underneath the runway were used to determine the time of foot-contact and lift-off events. All rats were trained to walk forward on the runway and to voluntarily step over the obstacle. During the training sessions, food was supplied to the rats to encourage them to move toward the black box. Reflective markers were placed on the shaved skin of the right hindlimb at the iliac crest, the greater trochanter, the knee joint, the lateral malleolus, and fifth metatarsal head (Fig. 1b). Movements were captured at 200 frames/s using a high-speed digital image camera system (HAS-220, DITECT, Inc., Tokyo, Japan). Movement analysis was limited to the sagittal plane parallel to the direction of locomotion. Custom-designed motion analysis software (DIPP-Motion Pro 2D, DITECT, Inc., Tokyo, Japan) was used to extract the two-dimensional coordinates of the different joint markers and to obtain angular excursions of the joints.

To collect the EMG data of each muscle during locomotion, EMG electrodes were implanted in different muscles of the hindlimbs under lightly anesthetized conditions. After recovery from anesthesia, the rats walked on a treadmill at speed of 0.4 m/s. We confirmed that the kinematics in the treadmill walking is consistent with the flat surface locomotion on the runway box. EMG activities were amplified (bandwidth, 150 Hz-10 KHz) and digitized with a data acquisition system at 10 KHz.

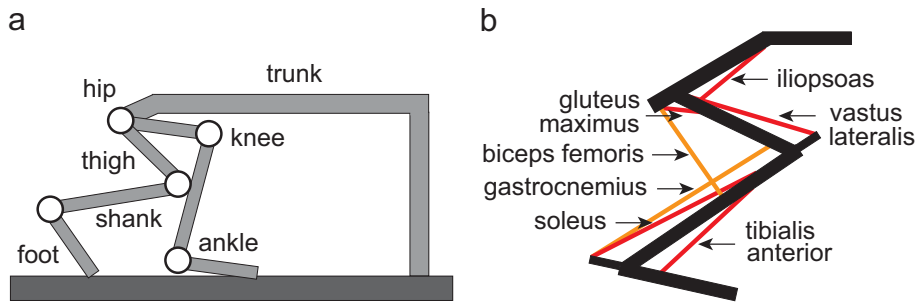


Fig. 2 Musculoskeletal model of the hindlimb of the rat. **a** Skeletal model. **b** Muscle model

Table 1 Physical parameters of the skeletal model

Parameter	Trunk	Thigh	Shank	Foot
Mass [g]	107	5.2	2.8	1.5
Length [mm]	69.6	18.5	27.2	17.7
MOI [$\times 10^2 \text{gmm}^2$]	1780	5.73	2.62	0.75

MOI: moment of inertia around the center of mass, where the center of mass was assumed to be at the middle of each segment

3 Model

3.1 Musculoskeletal model

Due to their geometrical similarity (Burkholder and Nichols 2004; Johnson *et al.* 2008), we developed the musculoskeletal model of the hindlimbs of the rat based on that of the cat (Ekeberg and Pearson 2005). The skeletal model consists of seven rigid links representing the trunk and hindlimbs (Fig. 2a). This model is two-dimensional and the walking behavior is constrained in the sagittal plane. When the thigh, shank, and foot are in a straight line and perpendicular to the trunk, the hip angle is 120° and the knee and ankle angles are both 180° . The joint angles increase as the joints are extending. We modeled the contact between the limb tips and the ground using viscoelastic elements. As we focus on the locomotion of the hindlimbs, the forelimbs are fixed on the trunk and slide on the ground without friction. We derived the equation of motion using Lagrangian equations and solved the equation of motion using the fourth-order Runge-Kutta method with time steps of 0.02 ms. Table 1 shows the physical parameters of the skeletal model determined from the measured anatomical data (see Section 2.1).

The muscle model has seven principal muscles for each hindlimb (IP, GM, VL, TA, SO, BF, and GA) (Fig. 2b). The moment arms of the muscles around the joints are constant, regardless of joint angles. A muscle receives command signals from the corresponding α -motoneuron and generates muscle tension depending on the force-length and force-velocity relationships. We used the mathematical model of

Table 2 Physical parameters of the muscle model

Parameter	IP	GM	VL	TA	SO	BF	GA
F_m^{\max} [N]	15.7	23.3	24.0	4.1	3.5	3.1	4.5
MA [mm]	4.5	2.3	3.2	5.1	6.0	2.5(h)	4.2(k)
						12.5(k)	6.0(a)

F_m^{\max} : maximum muscle tension, MA: moment arm of the muscle around the joint, IP: iliopsoas, GM: gluteus maximus, VL: vastus lateralis, TA: tibialis anterior, SO: soleus, BF: biceps femoris, GA: gastrocnemius, h: hip, k: knee, a: ankle

Ekeberg and Pearson (Ekeberg and Pearson 2005), composed of contractile and passive elements given by

$$F_m = F_m^{\max}(a_m \cdot F_m^l \cdot F_m^v + F_m^p) \quad (1)$$

where F_m ($m = \text{IP, GM, VL, TA, SO, BF, and GA}$) is the muscle tension, F_m^{\max} is the maximum muscle tension, a_m is the muscle activation ($a_m \geq 0$), F_m^l is the force-length relationship, F_m^v is the force-velocity relationship, and F_m^p is the passive component. We used the same equation for F_m^l , F_m^v , and F_m^p as in (Ekeberg and Pearson 2005). The muscle lengths were normalized by l_m^{\max} , which were set so that at a neutral posture with the hip at 65° , the knee at 90° , and the ankle at 100° , all uniarticular muscles had a length of 85% of l_m^{\max} and all biarticular muscles were at 75%. In addition, 2° of joint motion corresponded to 1% of muscle length change, except for the muscle GA, where 1.5° at the ankle or 4.5° at the knee were required. The muscle contractile velocities were normalized by $1.8l_m^{\max}$. Table 2 shows the physical parameters of the muscle model determined from the measured anatomical data (see Section 2.1). We determined the maximum muscle tension F_m^{\max} based on the measured PCSA and determined the moment arms from the center of the range of joint movement during locomotion.

Muscle activation a_m determines the muscle tension generated by the contractile element of the muscle, the dynamics of which is given by a low-pass filter (Yakovenko *et al.* 2004)

$$\dot{a}_m + \frac{1}{\tau_{\text{act}}} \left\{ \frac{\tau_{\text{act}}}{\tau_{\text{deact}}} + \left(1 - \frac{\tau_{\text{act}}}{\tau_{\text{deact}}} \right) u_m \right\} a_m = \frac{1}{\tau_{\text{act}}} u_m \quad (2)$$

where τ_{act} and τ_{deact} are activation and deactivation time constants (11 and 18 ms, respectively) and u_m is the output from the α -motoneuron determined by the model of the nervous system. Figure 3 shows the muscle activation generated by a rectangular α -motoneuron signal.

3.2 Nervous system model

In the spinal cord, command signals are projected to the α -motoneuron through interneurons by integrating signals from upper centers and sensory signals. For simplicity, we determined the out-

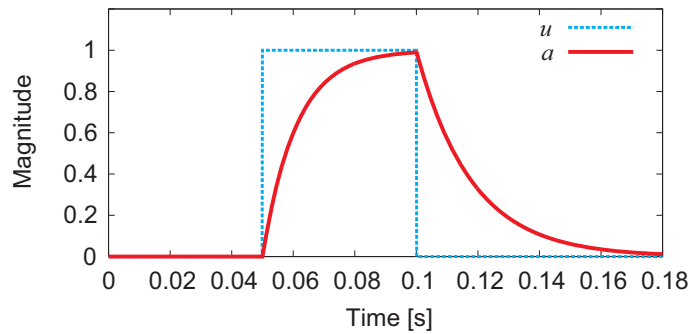


Fig. 3 Muscle activation a generated through the low pass filter to α -motoneuron signal u

put u_m from the α -motoneuron from the following three components by improving our previous model (Aoi *et al.* 2010): 1. movement control, which produces command signals in feedforward fashion at the spinal cord level to create periodic limb movements for forward motion and to create intended movements for obstacle avoidance (see Section 3.2.1 for periodic limb movements and Section 3.2.4 for obstacle avoidance); 2. phase modulation, which regulates timing to produce the feedforward signals of the movement control at the spinal cord level based on sensory signals (see Section 3.2.2 for phase resetting and Section 3.2.5 for interlimb coordination); and 3. posture control, which creates command signals in feedback fashion based on somatosensory information at the brainstem and cerebellar levels to regulate postural behavior (see Section 3.2.3).

3.2.1 Movement control for periodic limb movements

Physiological studies suggest that the CPGs in the spinal cord strongly contribute to rhythmic limb movement, such as locomotion (Grillner 1975; Orlovsky *et al.* 1999; Shik and Orlovsky 1976). The organization of CPGs remains unclear and various CPG models, such as the half-center model and the unit burst generator model, have been proposed (Guertin 2009; McCrea and Rybak 2008). However, physiological findings suggest that CPGs consist of hierarchical networks, including rhythm generator (RG) and pattern formation (PF) networks (Burke *et al.* 2001; Lafreniere-Roula and McCrea 2005; Rybak *et al.* 2006a; Rybak *et al.* 2006b). The RG network generates the basic rhythm and alters it by producing phase shift and rhythm resetting based on sensory afferents and perturbations (phase resetting). The PF network shapes the rhythm into spatiotemporal patterns of activated motoneurons through interneurons. CPGs separately control the locomotor rhythm and pattern of motoneuron activation in the RG and PF networks, respectively.

In the present study, we modeled the movement control with a two-layered hierarchical network model based on this physiological concept. For the RG model, we used two simple phase oscillators, each

of which produces a basic rhythm and phase information for the corresponding limb (Aoi *et al.* 2010). We denote ϕ_i ($i = \text{left, right}$) for the oscillator phase of the corresponding limb ($0 \leq \phi_i \leq 2\pi$). The oscillator phases follow the dynamics given by

$$\begin{aligned}\dot{\phi}_{\text{left}} &= \omega - K_\phi \sin(\phi_{\text{left}} - \phi_{\text{right}} - \pi) \\ \dot{\phi}_{\text{right}} &= \omega - K_\phi \sin(\phi_{\text{right}} - \phi_{\text{left}} - \pi)\end{aligned}\quad (3)$$

where ω is the basic frequency and K_ϕ is the gain parameter. We used $\omega = 8\pi$ rad/s to generate locomotion with a gait cycle of 250 ms. The second term on the right side indicates a function that maintains the interlimb coordination pattern so that the hindlimbs move out of phase.

Physiological studies also suggest the importance of the concept of muscle synergy, which explains the coordinated structure in muscle activities and is viewed as one means of coping with redundancy by decreasing the number of degrees of freedom. Many studies of muscle synergy have shown that although the EMG data recorded during locomotion are complex, they can be accounted for by the combination of only a small number of basic patterns (d'Avella and Bizzi 2005; d'Avella *et al.* 2003; Dominici *et al.* 2011; Ivanenko *et al.* 2004; Ivanenko *et al.* 2005; Ivanenko *et al.* 2006). In addition, the CPGs are suggested to manage the timing to produce such basic patterns based on kinematic events (Ivanenko *et al.* 2006). For the PF model, we prepared four rectangular pulses for the basic patterns of locomotion (Aoi *et al.* 2010; Jo and Massaquoi 2007; Jo 2008), whose timing of bursting initiation and duration depend on the oscillator phase ϕ from the RG model, and which are given by

$$P_i(\phi) = \begin{cases} 1 & \phi_i^{\text{Start}} < \phi \leq \phi_i^{\text{Start}} + \Delta\phi_i \\ 0 & \text{otherwise} \end{cases} \quad i = 1, \dots, 4 \quad (4)$$

where $P_i(\phi)$ ($i = 1, \dots, 4$) is the rectangular pulse, ϕ_i^{Start} the phase value when the rectangular pulse start to burst, and $\Delta\phi_i$ the duration of the rectangular pulse (Fig. 4). These four patterns are delivered to the α -motoneurons, and the output u_m^{Mov} of this movement control is given by

$$u_m^{\text{Mov}} = \sum_{i=1}^4 w_{m,i} P_i(\phi) \quad (5)$$

where $w_{m,i}$ ($i = 1, \dots, 4$) is the weighting coefficient for delivery of the four basic patterns to α -motoneurons ($w_{m,i} \geq 0$).

3.2.2 Phase modulation by phase resetting

As noted above, physiological findings suggest that the CPGs manage the timing to produce the basic patterns based on kinematic events (Ivanenko *et al.* 2006). In addition, the RG network in the CPGs modulates its basic rhythm by producing phase shifts and rhythm resetting based on

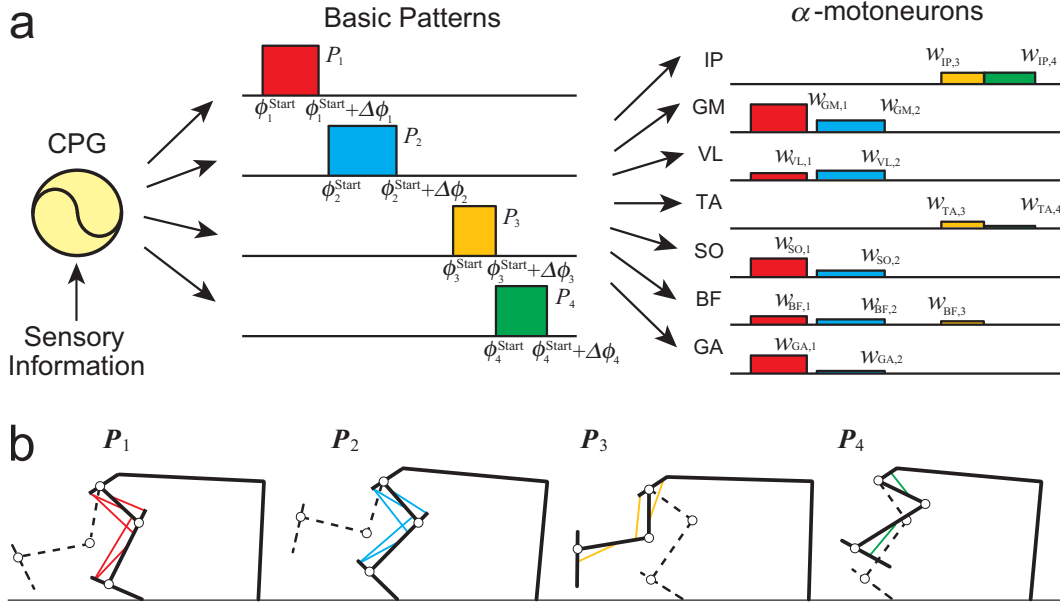


Fig. 4 The central pattern generator (CPG) produces basic patterns delivered to α -motoneurons and manages timing to produce the basic patterns based on sensory information. **a** Four rectangular pulses and command signals composed of combinations of four rectangular pulses. **b** Muscles activated by four rectangular pulses.

sensory information (phase resetting) (Lafreniere-Roula and McCrea 2005; Rybak *et al.* 2006a). As cutaneous afferents were observed to contribute to these phase shift and rhythm resetting behaviors (Duysens 1977; Schomburg *et al.* 1998), we modeled such phase resetting by resetting the oscillator phase ϕ_i based on foot-contact events (Aoi *et al.* 2010). To incorporate this, we modified, based on physiological evidence, the oscillator phase dynamics (3) by

$$\begin{aligned}\dot{\phi}_{\text{left}} &= \omega - K_{\phi} \sin(\phi_{\text{left}} - \phi_{\text{right}} - \pi) - (\phi_{\text{left}} - \phi^{\text{Contact}}) \delta(t - t_{\text{left}}^{\text{Contact}} - \tau^{\text{Contact}}) \\ \dot{\phi}_{\text{right}} &= \omega - K_{\phi} \sin(\phi_{\text{right}} - \phi_{\text{left}} - \pi) - (\phi_{\text{right}} - \phi^{\text{Contact}}) \delta(t - t_{\text{right}}^{\text{Contact}} - \tau^{\text{Contact}})\end{aligned}\quad (6)$$

where $\delta(\cdot)$ is Dirac's delta function, t_i^{Contact} ($i = \text{left}, \text{right}$) is the time when the foot lands on the ground, and ϕ^{Contact} is the phase value to be reset when the foot touches the ground. The third term of the right side constitutes the phase resetting, which will reset the oscillator phase ϕ_i to ϕ^{Contact} when the foot touches the ground to modulate the timing to produce the basic patterns and the locomotor rhythm based on sensory information. This phase resetting depends on the tactile sensor on the foot and the delay in the spinal cord receiving the sensory signal. We set the transmission delay τ^{Contact} at 10 ms, which we determined based on the physiological observation that the electrical stimulation of the hindlimb muscle induces short-latency (about 12 ms) evoked potentials in the cerebellar cortex

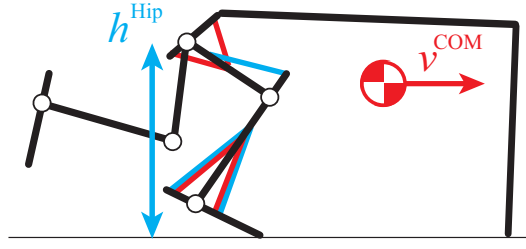


Fig. 5 Posture control based on hip height and horizontal center of mass (COM) velocity

via the spinocerebellar tract (Muramatsu *et al.* 2009). Note that this phase resetting modulates the locomotor phase based on the information of the corresponding ipsilateral limb.

3.2.3 Posture control

At the levels of the brainstem and cerebellum, command signals are produced to regulate postural behavior based on somatosensory information. For the locomotor behavior of the rat, it is crucial to maintain the hip height and forward velocity during locomotion (Fig. 5). For simplicity, we focused on these two factors for posture control.

Cerebellar activity is suggested to encode limb axis length and orientation, that is, the position of the limb endpoint relative to the root and its direction (Bosco and Poppele 2001; Casabona *et al.* 2003; Casabona *et al.* 2004; Poppele *et al.* 2002; Poppele and Bosco 2003). Thus, information about the hip height of the supporting limb is likely represented at the level of the cerebellum. For the postural control of the hip height, we used simple feedback control by muscles VL, TA, and SO of the standing limb to maintain the hip height during locomotion,

$$p_m^{\text{Hgt}} = \begin{cases} -K_m^{\text{Hgt}}(h^{\text{Hip}} - \hat{h}^{\text{Hip}}) - D_m^{\text{Hgt}}\dot{h}^{\text{Hip}} & \text{when } f^{\text{GRF}} > 0 \\ 0 & \text{otherwise} \end{cases} \quad (7)$$

where h^{Hip} and \dot{h}^{Hip} are the hip height and its rate, \hat{h}^{Hip} is the reference height, K_m^{Hgt} and D_m^{Hgt} are the gain parameters ($K_m^{\text{Hgt}} = D_m^{\text{Hgt}} = 0$ when $m \neq \text{VL, TA, or SO}$), and f^{GRF} is the vertical ground reaction force.

Feedback control using the center of mass (COM) and its velocity has been used to investigate the stability mechanism during quiet standing for humans and animals (Asai *et al.* 2009; Lockhart and Ting 2007; Masani *et al.* 2003; Masani *et al.* 2006; Maurer and Peterka 2005; Peterka 2000; Welch and Ting 2008). The COM velocity represents the locomotion speed and the COM and its velocity are thought to be controlled in the nervous system during locomotion (Chonga *et al.* 2009). For the postural control of

COM velocity, we used simple feedback control by muscles IP, GM, TA, and SO of the standing limb,

$$p_m^{\text{COM}} = \begin{cases} -K_m^{\text{COM}}(v^{\text{COM}} - \hat{v}^{\text{COM}}) & \text{when } f^{\text{GRF}} > 0 \\ 0 & \text{otherwise} \end{cases} \quad (8)$$

where v^{COM} is the COM velocity, \hat{v}^{COM} is its desired value, and K_m^{COM} is the gain parameter ($K_m^{\text{COM}} = 0$ when $m \neq \text{IP, GM, TA, or SO}$).

The summation of these two elements produces the command signal of posture control. As this posture control is managed at the brainstem and cerebellar levels, the command signals are delayed and the output u_m^{Pos} of this posture control is given by

$$u_m^{\text{Pos}}(t) = p_m^{\text{Hgt}}(t - \tau^{\text{Somato}} - \tau^{\text{Descend}}) + p_m^{\text{COM}}(t - \tau^{\text{Somato}} - \tau^{\text{Descend}}) \quad (9)$$

where τ^{Somato} and τ^{Descend} are the delays in receiving transmission of somatosensory information at the brainstem and cerebellar levels and sending the command signal to the spinal cord level, respectively. We used $\tau^{\text{Somato}} + \tau^{\text{Descend}} = 15$ ms based on (Muramatsu *et al.* 2009).

3.2.4 Strategy for stepping over an obstacle

In contrast to usual locomotion, obstacle avoidance is a skillful intentional movement, in which the rat must recognize the dimensions of the obstacle and determine how to control its limbs to avoid a collision while maintaining its posture. This task requires highly coordinated control of spatiotemporal patterns of command signals. Analysis of muscle synergy has shown that the addition of another pattern to the basic patterns of locomotion explains the muscle activities for obstacle avoidance (Ivanenko *et al.* 2005; Ivanenko *et al.* 2006), which means that this additional pattern controls the intralimb (intersegmental) coordination of the limb movement. Jo (2008) evaluated this hypothesis for stepping over an obstacle with one leg based on a neuromusculoskeletal model of human locomotion.

For obstacle avoidance during locomotion, the leading limb steps over an obstacle and the trailing limb follows it and clears the obstacle, as shown in Fig. 6. Therefore, to complete this task, both leading and trailing limbs must step over an obstacle without colliding with it. In the present study, we conducted a computer simulation of stepping over an obstacle during locomotion by the hindlimbs without modulating the stride length before obstacle avoidance; we neglected the collision of the forelimbs with the obstacle. As the tip of the leading limb is distant from the obstacle when it lifts from the ground, it steps over the obstacle at the posterior half of the swing phase (Fig. 6). On the other hand, the tip of the trailing limb is closer to the obstacle at its liftoff and clears the obstacle at the anterior half of the swing phase. Thus, the movement of the leading limb differs from that of the trailing limb during the obstacle avoidance, meaning that the roles of the two limbs are not identical.

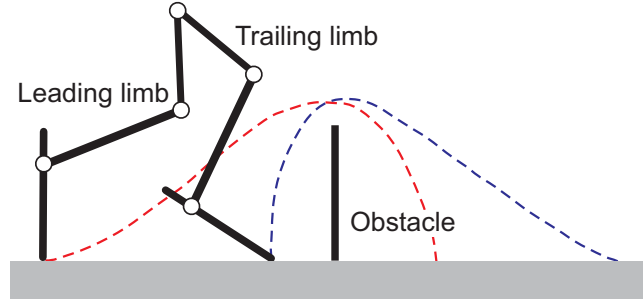


Fig. 6 Stepping over an obstacle by the leading and trailing limbs

To model stepping over an obstacle, we prepared an additional rectangular pulse for each leading and trailing limb, and used them only once for the obstacle avoidance. The additional rectangular pulse $P_{\text{Lead}}(\phi_{\text{Lead}})$ for the leading limb and $P_{\text{Trail}}(\phi_{\text{Trail}})$ for the trailing limb are given by

$$P_i(\phi_i) = \begin{cases} 1 & \phi_i^{\text{Start}} < \phi_i \leq \phi_i^{\text{Start}} + \Delta\phi_i \\ 0 & \text{otherwise} \end{cases} \quad i = \text{Lead, Trail} \quad (10)$$

where ϕ_i^{Start} ($i = \text{Lead, Trail}$) is the phase value when the rectangular pulse starts to burst and $\Delta\phi_i$ is the duration of the rectangular pulse. In this study, we used the left limb for the leading limb and the right for the trailing limb in each trial. To step over the obstacle, the rat must not only swing the limb more than usual, but also support the body by the contralateral limb. Therefore, the additional rectangular pulse contributes to the contralateral supporting limb as well as to the ipsilateral swinging limb. The additional rectangular pulse is delivered to the α -motoneurons, and the outputs $u_{m,\text{Ipsi}}^{\text{Lead}}$ for the leading limb, $u_{m,\text{Contra}}^{\text{Lead}}$ for the limb contralateral to the leading limb, $u_{m,\text{Ipsi}}^{\text{Trail}}$ for the trailing limb, and $u_{m,\text{Contra}}^{\text{Trail}}$ for the limb contralateral to the trailing limb are given by

$$\begin{aligned} u_{m,\text{Ipsi}}^{\text{Lead}} &= w_{m,\text{Lead}}^{\text{Ipsi}} P_{\text{Lead}}(\phi_{\text{Lead}}), & u_{m,\text{Contra}}^{\text{Lead}} &= w_{m,\text{Lead}}^{\text{Contra}} P_{\text{Lead}}(\phi_{\text{Lead}}) \\ u_{m,\text{Ipsi}}^{\text{Trail}} &= w_{m,\text{Trail}}^{\text{Ipsi}} P_{\text{Trail}}(\phi_{\text{Trail}}), & u_{m,\text{Contra}}^{\text{Trail}} &= w_{m,\text{Trail}}^{\text{Contra}} P_{\text{Trail}}(\phi_{\text{Trail}}) \end{aligned} \quad (11)$$

where $w_{m,\text{Lead}}^{\text{Ipsi}}$, $w_{m,\text{Lead}}^{\text{Contra}}$, $w_{m,\text{Trail}}^{\text{Ipsi}}$, and $w_{m,\text{Trail}}^{\text{Contra}}$ are the weighting coefficients for delivering the additional rectangular pulses to α -motoneurons (Fig. 7).

After our model produced steady walking, we added these additional inputs only once for the obstacle avoidance. As these additional inputs change the kinematics of the leading and trailing limbs, we calculated the height of the obstacle that our model steps over without collision from the resultant simulated kinematics of the leading and trailing limbs, where we assumed that the width of the obstacle is negligible, that is, we modeled the obstacle as a zero-width bar in the sagittal plane.

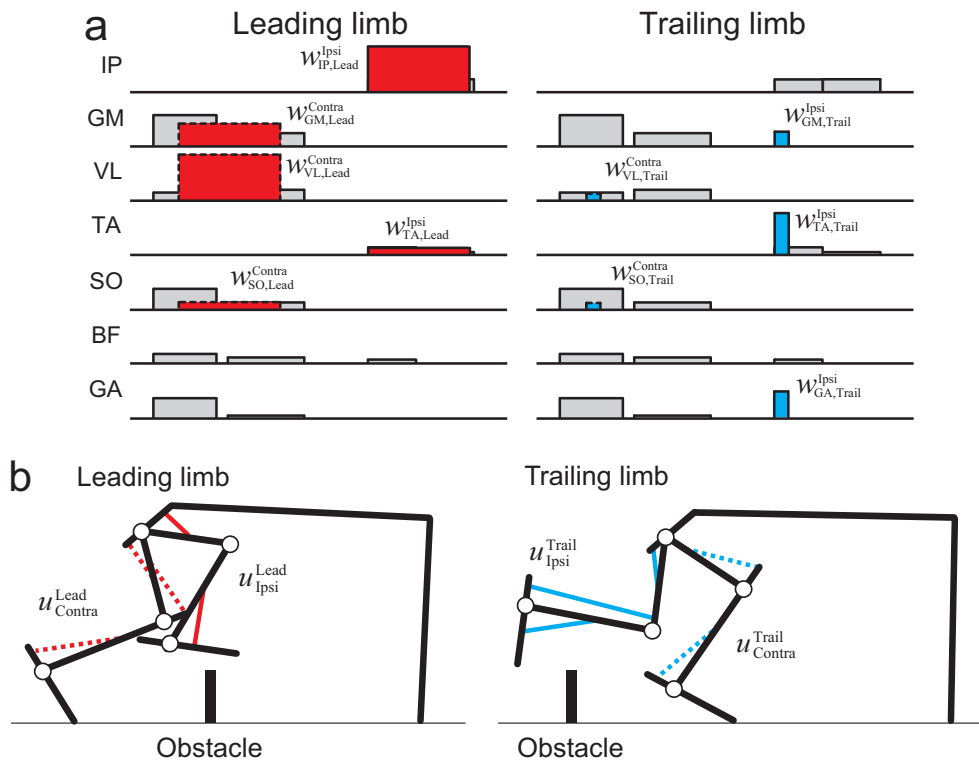


Fig. 7 Additional rectangular pulses for obstacle avoidance by the leading and trailing limbs. **a** Command signals are delivered to the α -motoneurons for swinging and supporting limbs. **b** Muscles activated by the additional rectangular pulses. Solid and dotted lines correspond to the contributions to the swinging and supporting limbs, respectively.

3.2.5 Regulation of interlimb coordination pattern during obstacle avoidance

As explained in the previous section, supporting the body by the contralateral limb is important for obstacle avoidance. When the leading or trailing limb starts stepping over an obstacle without support from the contralateral limb, obstacle avoidance fails; thus, interlimb coordination between the ipsilateral and contralateral limbs while stepping over an obstacle is crucial for the success of the trial.

To control this interlimb coordination, we regulated the phase of the ipsilateral limb by setting $\dot{\phi}_i = 0$ ($i = \text{Lead, Trail}$) when $\phi_i \geq \phi_i^{\text{Start}}$ and the ground reaction force of the contralateral limb is zero; that is, the contralateral limb does not support the body. This aimed to delay the additional rectangular pulse for stepping over an obstacle until the contralateral limb supported the body. For this sensory regulation, we used a transmission delay of 10 ms for the tactile sensory information of the contralateral limb.

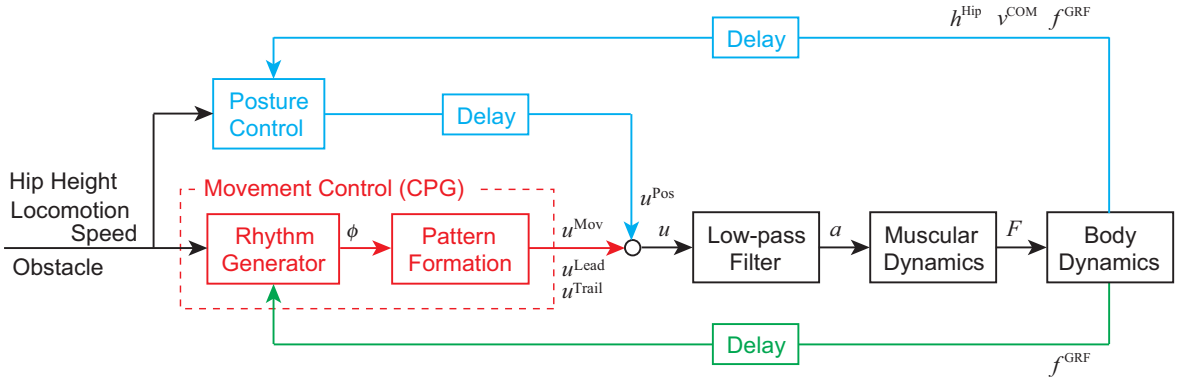


Fig. 8 Nervous system model. Red blocks and arrows indicate movement control; blue, posture control; and green, phase modulation.

3.2.6 Output from the α -motoneuron

Because the analysis of muscle synergy has shown that the combination of basic patterns explains the large part of muscle activation patterns (Ivanenko *et al.* 2004; Ivanenko *et al.* 2005; Ivanenko *et al.* 2006) as explained above, we constructed the output u from the α -motoneuron by a summation of the outputs from the controllers as follows

$$u_m = u_m^{\text{Mov}} + u_m^{\text{Pos}} + u_m^{\text{Lead}} + u_m^{\text{Trail}} \quad (12)$$

Figure 8 shows the flow of information in our nervous system model.

3.2.7 Parameter determination

Our nervous system model has 27 parameters for locomotion and 14 parameters for obstacle avoidance (see Appendix A). We determined these using the following two-step approach in a similar way to that described in our previous work (Aoi *et al.* 2010). Here note that we did not focus on optimizing these parameters, but rather on the emergence of adaptive functions during locomotion and obstacle avoidance through neuro-mechanical interactions.

In the first step, we used empirical, two-dimensional position data from markers attached to the rat during locomotion (see Section 2.2). We calculated joint kinematics by adapting the position data to our skeletal model, and achieved the desired length profile of each muscle for one gait cycle. We set muscle activation a_m using a proportional and derivative (PD) feedback control relative to muscle length to follow the desired length instead of equation (2), and performed computer simulation of the rat locomotion (Kondo *et al.* 2010). We then conducted principal component analysis (PCA) of the resultant muscle activations and determined that four rectangular pulses ($P_{1...4}$) would sufficiently model the basic patterns of movement control for periodic limb movements. We determined parame-

ters ϕ_i^{Start} , $\Delta\phi_i$, and $w_{m,i}$ ($i = 1, \dots, 4$) of the four rectangular pulses from the PCA and determined parameters \hat{h}^{Hip} and \hat{v}^{COM} for posture control from the resultant walking behavior. We also used measured kinematic data from obstacle avoidance by the rat (see Section 2.2) and determined parameters ϕ_i^{Start} , $\Delta\phi_i$, $w_{m,i}^{\text{Ipsi}}$, and $w_{m,i}^{\text{Contra}}$ ($i = \text{Lead, Trail}$) for the additional rectangular pulses for the obstacle avoidance.

In the next step, we incorporated the movement and posture controls for locomotion. We determined muscle activation a_m as the summation of the PD feedback control used in the first step and the command signals from the movement and posture controls through the low-pass filter (2). We determined and modulated parameters $w_{m,i}$ for movement control and the gain parameters for posture control by trial and error, while decreasing the gain parameters in the PD feedback control until they vanished, and muscle activations were determined by the movement and posture controls alone. After we determined the parameters for locomotion, we modulated $w_{m,i}^{\text{Ipsi}}$ and $w_{m,i}^{\text{Contra}}$ to achieve obstacle avoidance.

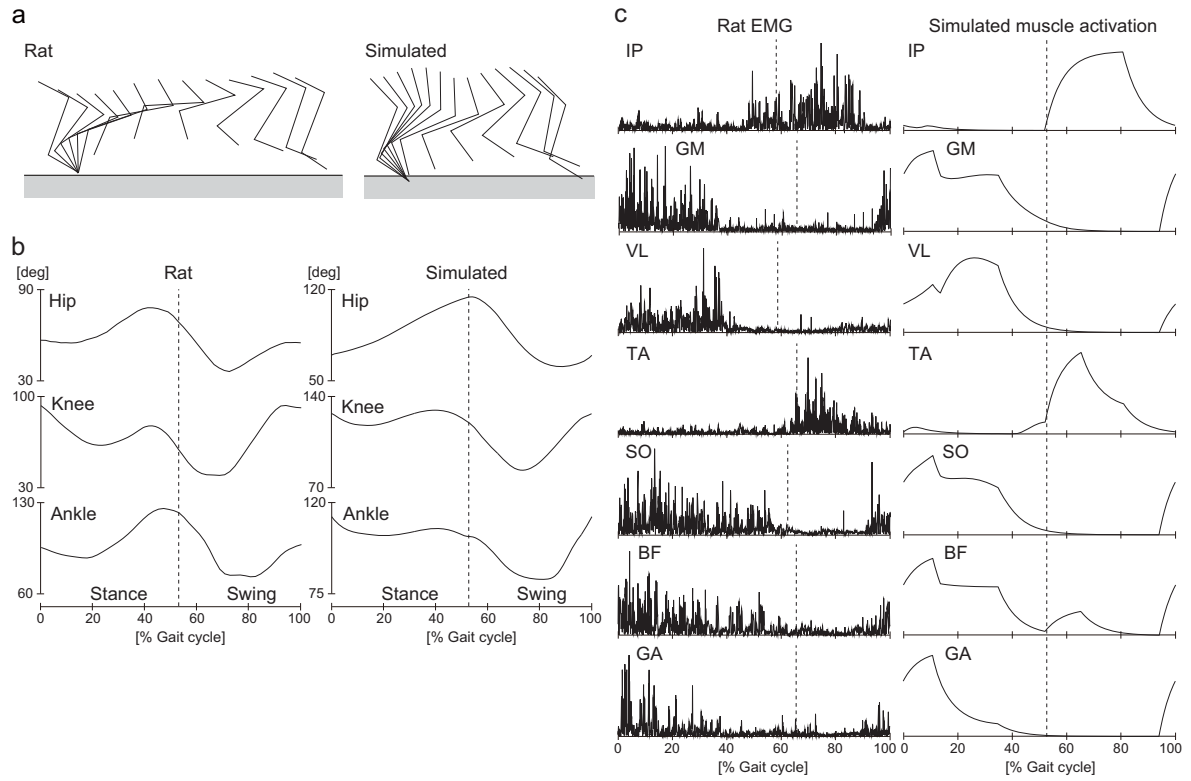


Fig. 9 Results of simulated locomotion compared with actual data from rats. **a** Rat (left) and simulated (right) walking behavior illustrated by stick diagrams. **b** Joint angles over the course of one walking cycle. The vertical lines indicate the point when the foot was off the ground. **c** Muscle activation patterns of the seven muscles derived from rat EMG data (left) and from computer simulations (right). Kinematic data were collected during locomotion over a flat surface and EMG data during treadmill locomotion. IP: iliopsoas, GM: gluteus maximus, VL: vastus lateralis, TA: tibialis anterior, SO: soleus, BF: biceps femoris, GA: gastrocnemius.

4 Results

4.1 Generation of locomotion

First, we conducted a computer simulation based on our neuromusculoskeletal model and produced steady walking without using additional rectangular pulses for obstacle avoidance. Figure 9 shows the simulation results compared with the measured data. Although the hip and knee joints of the simulated walking are more extended and the stride length is shorter than the empirical data, these comparisons indicate that the computer simulation successfully established results similar to rat locomotion despite the limitations associated with the use of simple rectangular pulses for movement control. The parameters used for locomotion in the nervous system model are presented in Appendix A.1.

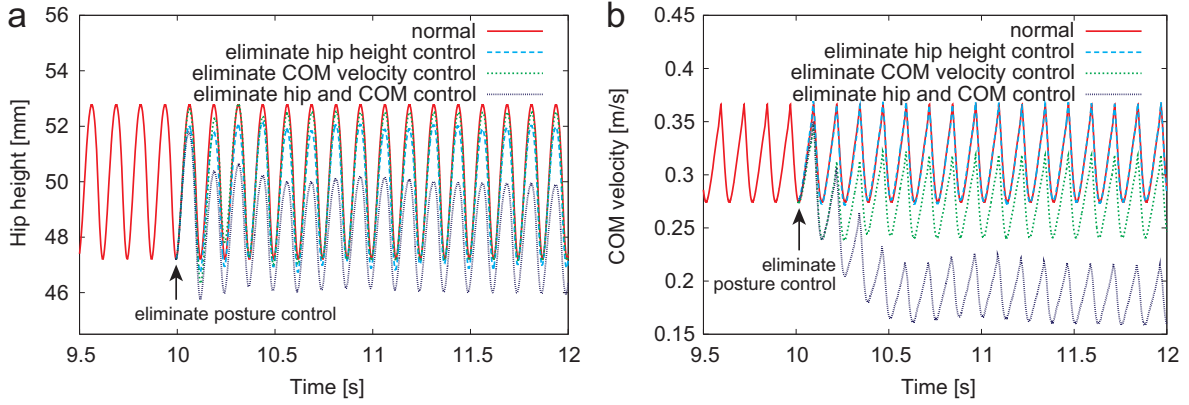


Fig. 10 Contribution of posture control to hip height (a) and center of mass (COM) velocity (b) during walking

4.2 Contribution of posture control

Muscle activation patterns are produced by command signals from the movement and posture controls. We calculated the contributions of posture control during steady walking for muscles IP, GM, VL, TA, and SO from the results of Fig. 9 as follows

$$\frac{\int_{t_0}^{t_0+\tau^{\text{Cycle}}} |u_m^{\text{Pos}}(t)| dt}{\int_{t_0}^{t_0+\tau^{\text{Cycle}}} \{|u_m^{\text{Mov}}(t)| + |u_m^{\text{Pos}}(t)|\} dt} \quad (13)$$

where τ^{Cycle} is the duration of one gait cycle ($= 250$ ms), and found them to be 1, 2, 2, 3, and 3%, respectively. Although these contributions are relatively small, they are important in generating walking. When we eliminated posture control for the hip height during locomotion, it decreased and fluctuated, because adequate supporting forces could not be produced (Fig. 10a). Abolition of posture control for COM velocity decreased walking speed, because adequate propulsive forces could not be obtained (Fig. 10b). When we eliminated the posture control for both the hip height and COM velocity, our model finally fell down.

4.3 Stepping over an obstacle

Next, we conducted computer simulation of obstacle avoidance using additional rectangular pulses. Figure 11 shows stick diagrams of the results. When walking was calculated from the simulated limb kinematics shown in Fig. 9, our model could clear an obstacle of only 7 mm; however, when additional inputs were added to the model, it stepped over an obstacle of 17 mm. After our model stepped over

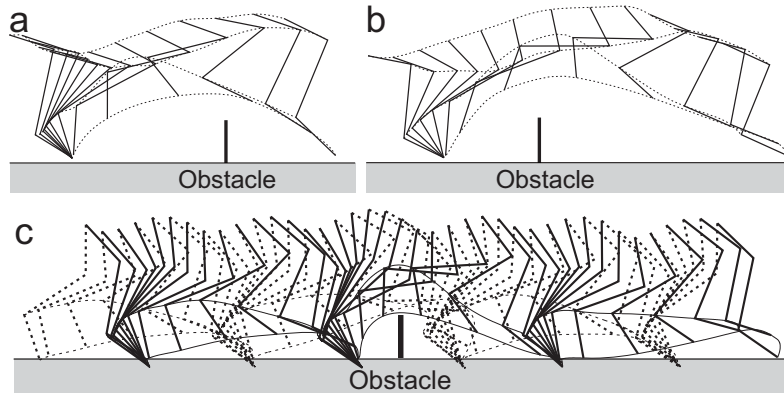


Fig. 11 Stick diagrams illustrating during obstacle avoidance. **a, b** Measured kinematics of the leading (**a**) and trailing (**b**) limbs. **c** Simulated obstacle avoidance behavior.

the obstacle, the walking behavior soon recovered without falling over. The parameters for this obstacle avoidance are presented in Appendix A.2.

4.4 Contribution of phase regulation based on phase resetting and interlimb coordination

To investigate the contribution of phase modulation based on phase resetting and interlimb coordination to obstacle avoidance, we used various magnitudes of the additional rectangular pulses and examined what height of obstacle our model could step over without falling down. In particular, we compared four cases; 1. without phase modulation; 2. with phase modulation based on interlimb coordination; 3. with phase modulation based on phase resetting; and 4. with phase modulation based on both phase resetting and interlimb coordination.

Figure 12 shows the heights of the obstacle that our model cleared with various magnitudes of the additional inputs. When we did not use phase modulation based on phase resetting, our model stepped over an obstacle of at best 8 mm (40% of additional inputs), but easily fell down after stepping over higher obstacles (Fig. 13). The phase regulation based on interlimb coordination allowed our model to clear higher obstacles. Although the model with the phase resetting-based modulation also stepped over higher obstacles, it required higher magnitudes of additional inputs than the model with both phase resetting and interlimb coordination, which cleared high obstacles using small additional inputs without falling over after stepping over the obstacles.

4.5 Parameter sensitivity of our results

To confirm the robustness of our findings, we investigated the parameter sensitivity of our results. Because gait cycle duration is a crucial factor in determining the locomotor behavior, we used various

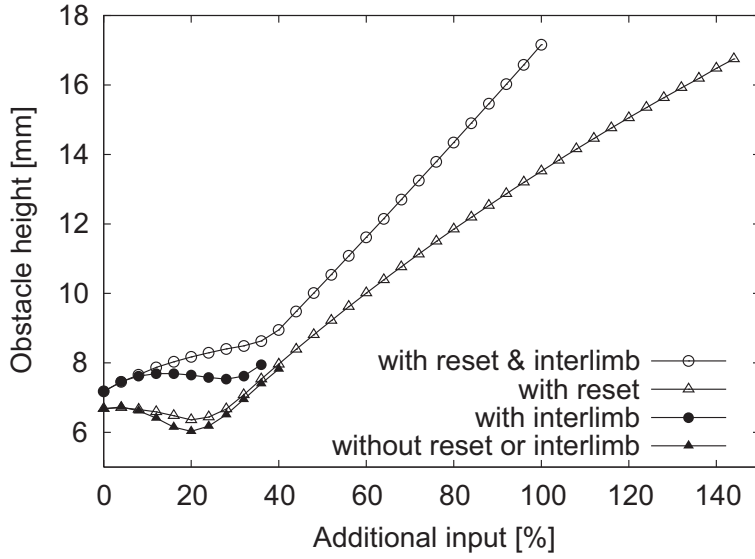


Fig. 12 Comparison of obstacle heights with and without phase regulation based on phase resetting and interlimb coordination

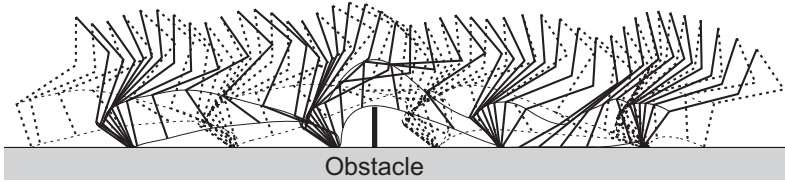


Fig. 13 Simulated behavior of stepping over an obstacle without phase modulation based on phase resetting (100% of additional inputs) followed by falling down

values for the duration of the gait cycle, that is, we used various values for ω in (3). Since the durations of the rectangular pulses in the movement control and the locomotion speed depend on the gait cycle duration, we modified the weighting coefficient $w_{m,i}$ ($i = 1, \dots, 4$) of the movement control in (5) and the reference parameter \hat{v}^{COM} of the posture control for the COM velocity in (8) to establish similar locomotor behavior for various gait cycle durations. Specifically, we changed these parameters uniformly in accordance with the gait cycle duration. In this analysis, we compared three cases, 1. we used the additional inputs for obstacle avoidance and used the phase regulations based on phase resetting and interlimb coordination, 2. we used the additional inputs but did not use the phase regulations, and 3. we did not use the additional inputs. Figure 14 shows the obstacle height that our model cleared. This figure shows that the additional inputs and sensory regulations contribute to stepping over higher obstacles, regardless of the duration of the gait cycle. When the gait cycle duration greatly changes, the uniform modification of the parameters is not sufficient to establish steady walking and stepping over an obstacle and a more sophisticated parameter search is required. We intend to investigate this in future studies.

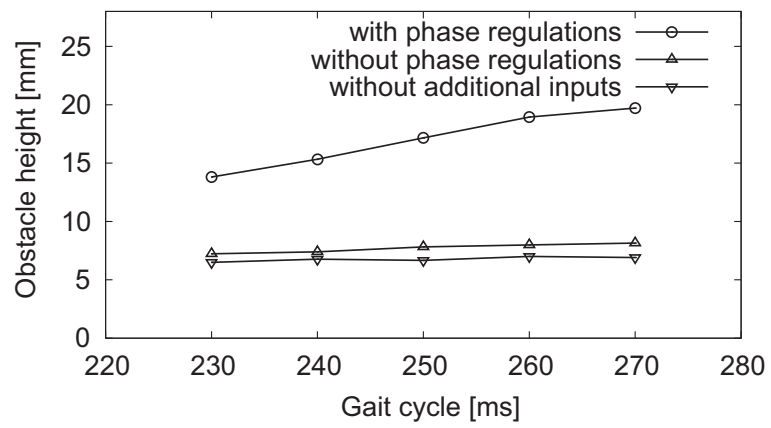


Fig. 14 Comparison of the cleared obstacle height for various gait cycle durations

5 Discussion

5.1 Sensory regulation during obstacle avoidance in locomotion

For successful obstacle avoidance during locomotion, two factors are crucial; the leading and trailing limbs must clear the obstacle without collision and the walking behavior must recover soon after stepping over the obstacle (Taga 1998). As the obstacle height increases, the toe heights of the leading and trailing limbs must also be increased, which disturbs postural control and causes instability and falling down. Therefore, stepping over a high obstacle and recovering soon after are not consistent. In the present study, we incorporated sensory regulation models based on phase resetting using the foot-contact information of the ipsilateral limb and based on interlimb coordination using the foot-contact information of the contralateral limb. Our simulation results show that interlimb coordination efficiently contributes to stepping over a high obstacle and that phase resetting contributes to a quick recovery after stepping over the obstacle.

5.2 Roles of phase modulation based on interlimb coordination

Phase modulation based on interlimb coordination allowed our model to clear a high obstacle with only a small additional input (Fig. 12). As the additional input for the leading limb increases, the toe height of the leading limb increases and its contact with the surface is delayed. When the delay is longer than the onset of the additional input for the trailing limb, our model starts stepping over the obstacle without support from the contralateral limb and the performance decreases, as shown in the case without phase modulation based on interlimb coordination in Fig. 12. This is verified by the relationship between the times for the foot-contact of the leading limb and the onset of the additional input to the trailing limb as shown in Fig. 15, calculated from the results in Fig. 12.

Although the phase modulation based on this interlimb coordination increased the obstacle avoidance performance (Fig. 12), it shifted the relative phase of the four rectangular pulses for the basic patterns of locomotion between the limbs from being out of phase. The phase modulation by phase resetting also induces this shift of the relative phase. Because this shift causes instability and falling over during walking, the relative phase should return to being out of phase after stepping over an obstacle. The gain parameter K_ϕ in (3) manages the regulation of this relative phase. When we used a large value for this K_ϕ , the relative phase quickly returned to being out of phase. The obstacle height that our model cleared without falling down depended on K_ϕ , as shown in Fig. 16. When we used a small value for K_ϕ , our model easily fell down after stepping over a high obstacle; however, when K_ϕ

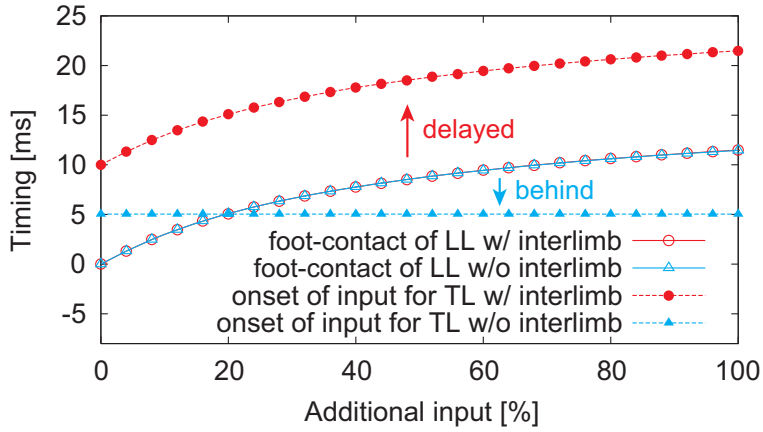


Fig. 15 Relationship between times for foot-contact of the leading limb (LL) and onset of additional input to the trailing limb (TL). These results use phase modulation based on phase resetting.

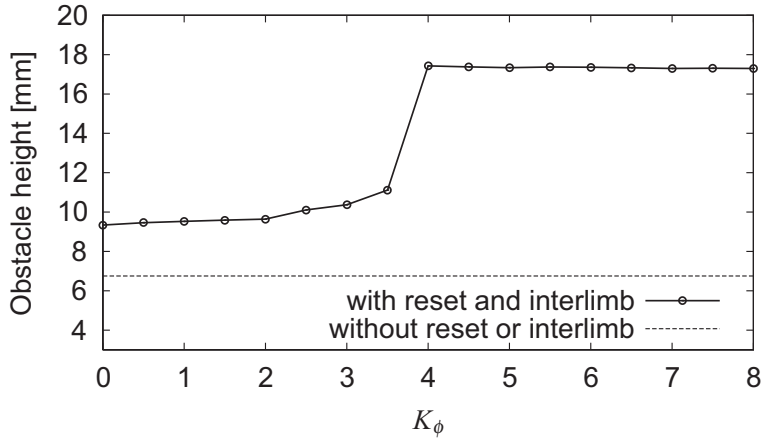


Fig. 16 Relationship between obstacle height cleared and magnitude of the gain parameter K_ϕ

was larger than 4.0, our model stepped over higher obstacles. This demonstrates the importance of adequate control of interlimb coordination during locomotion and obstacle avoidance.

A previous study in rats showed that the footfall sequence during stepping over an obstacle demonstrated proper modification in place of the fundamental sequence during overground locomotion (Sato *et al.* 2012), suggesting that rats control their interlimb coordination for obstacle avoidance. Our results are consistent with this observation.

5.3 Roles of phase modulation based on phase resetting

Although physiological evidence showed that locomotor rhythm and phase are modulated by phase shifts and rhythm resetting produced based on sensory afferents and perturbations (Conway *et al.* 1987; DuySENS and Pearson 1980; Guertin *et al.* 1995; Lafreniere-Roula and McCrea 2005; Schomburg *et al.* 1998),

such rhythm and phase modulations have been investigated, for the most part, during fictive locomotion in cats, and their functional roles during actual locomotion remain largely unclear. However, spinal cats produce locomotor behaviors on treadmills with gait changes that depend on the belt speed (Forssberg and Grillner 1973; Orlovsky *et al.* 1999), suggesting that the tactile sensory information between their feet and the belt influences the locomotion phase and rhythm generated by the CPG (Duysens *et al.* 2000). In addition, cutaneous afferents were observed to contribute to phase resetting (Duysens 1977; Schomburg *et al.* 1998). Neuromusculoskeletal models of biological systems demonstrated that phase resetting contributes to the generation of adaptive walking (Aoi *et al.* 2010; Yakovenko *et al.* 2004; Yamasaki *et al.* 2003a; Yamasaki *et al.* 2003b).

The spatiotemporal patterns of command signals determine locomotor behavior and phase resetting manages the temporal modulation based on foot-contact events. Even if the timing of the foot-contact event is disturbed due to obstacle avoidance, phase resetting regulates the timing to generate command signals based on the event. Early foot-contact induces a phase shift of periodic command signals to interrupt the locomotor rhythm, and delayed foot-contact results in a phase shift of periodic command signals to prolong the locomotor rhythm. Phase resetting creates various phase profiles and locomotor rhythms depending on the situation, thus improving the stability and robustness of locomotion. Our demonstration of the contribution of this phase resetting to quick recovery is consistent with our previous simulation results of human walking (Aoi *et al.* 2010).

The contributions of phase shift based on sensory information to the generation of adaptive locomotion have been investigated using neuromusculoskeletal models. Ekeberg and Pearson (2005) delineated four phases (touchdown, stance, liftoff, and swing) for command signals of the hindlimbs of cats and used the foot-contact information at touchdown to change the phase from the touchdown to stance phase, as we did in our model. They showed that the transition from the stance to liftoff phase based on the unloading of the hindlimb contributes to adaptive locomotor behavior. Our previous work on human locomotion (Aoi *et al.* 2012) confirmed such contribution of the phase transition based on the unloading of the leg. However, the present study in rats used only the sensory regulation model based on the foot-contact information to simplify and clarify the sensory-motor coordination regarding phase resetting and interlimb coordination.

5.4 Physiological concept of muscle synergy

Humans and animals produce adaptive movements from the combination of a great deal of degrees of freedom, from which they must solve the redundancy problem. Physiological findings suggest the importance of muscle synergies for controlling movements (d'Avella and Bizzi 2005; d'Avella *et al.* 2003;

Drew *et al.* 2008; Ivanenko *et al.* 2005; Latash 2008; Ting and Macpherson 2005; Todorov and Jordan 2002), which are viewed as one solution to handle the redundancy problem. Muscle synergy is related to the co-variation of muscle activities. Humans and animals share some basic patterns for producing muscle activation patterns among various movements (e.g., the jump, swim, and walk patterns of frogs and the walk, obstacle avoidance, kick motion, and run of humans) and produce these various movements by adding other patterns (Cappellini *et al.* 2006; d’Avella and Bizzi 2005; Ivanenko *et al.* 2004; Ivanenko *et al.* 2005; Ivanenko *et al.* 2006). This means that some degrees of freedom are functionally connected depending on the task, which reduces the number of degrees of freedom and solves the problem of motor redundancy.

CPGs were suggested to produce such basic patterns in a feedforward fashion to create various movements, and adding another pattern to the basic patterns for locomotion explains the motor control of stepping over an obstacle (Ivanenko *et al.* 2005; Ivanenko *et al.* 2006). Based on this physiological finding, we prepared a simple rectangular pulse model, inspired from a previous model (Jo 2008). In addition, because sensory regulations of the timing to produce the basic patterns are crucial (Ivanenko *et al.* 2006), we employed the foot-contact information of the ipsilateral and contralateral limbs to modulate the timing; thereby demonstrating by computer simulation the contribution of these sensory regulations during obstacle avoidance during locomotion.

5.5 Limitations of our simulation model

In the present study, we modeled the rat nervous system in a simple fashion using only four rectangular pulses for the movement control of locomotion and one additional pulse for the obstacle avoidance, which limited the shapes of the command signals. Furthermore, we employed control mechanisms based only on the hip height and COM velocity for posture control. Although the simulation results of such simple modeling differed to some extent from actual rat locomotion and obstacle avoidance, our results were similar to the features of these behaviors both kinematically and kinetically (Figs. 9 and 11), and clearly demonstrated the contribution of sensory regulation based on interlimb coordination and phase resetting to successful and efficient obstacle avoidance (Fig. 12).

We confined our musculoskeletal model to two dimensions and did not incorporate the forelimbs or phalangeal part of the hindlimb feet. In particular, because the forelimbs support more load that is redistributed between the left and right limbs when raising the hindlimb, the forelimbs would also play a significant role in stepping over a high obstacle and in quickly recovering after obstacle avoidance. Now that the basics have been formulated, we intend to employ a more sophisticated and plausible model to further examine these contributions.

Although we focused on the implementation of stepping over an obstacle using additional inputs, the modification of walking behavior during the approach phase prior to reaching the obstacle is also important (Austin *et al.* 1999; Chou and Draganich 1998; Patla and Greig 2006; Sato *et al.* 2012; Taga 1998). During obstacle avoidance in rat locomotion, the toe height increases depending on obstacle heights and the final stride length and swing phase duration of the trailing limb are significantly shorter than other steps during the approach phase. However, the horizontal distance between the toe and obstacle just prior to stepping over it is not influenced by the obstacle height (Sato *et al.* 2012). In future studies, we intend to incorporate such a regulation model during the approach phase to investigate its functional role in appropriate preparation for stepping over an obstacle.

A Parameters in the nervous system model

A.1 Parameters for locomotion

To determine the parameters for the movement control of periodic limb movements, we first calculated the length profile of each muscle for one gait cycle from the joint kinematic data of rats during locomotion and then conducted the computer simulation by determining the muscle activation a_m using PD feedback control relative to muscle length to follow the calculated length profile instead of Eq. (2), similar to the method used in our previous work (Aoi *et al.* 2010). Based on the principal component analysis (PCA) for the simulated muscle activation patterns, we determined the parameters for the four basic patterns ($CPG_{1...4}$) as follows: $\phi_1^{\text{Start}} = 5.9$ rad, $\phi_2^{\text{Start}} = 0.85$ rad, $\phi_3^{\text{Start}} = 3.26$ rad, $\phi_4^{\text{Start}} = 4.09$ rad, $\Delta\phi_1 = 1.06$ rad, $\Delta\phi_2 = 1.33$ rad, $\Delta\phi_3 = 0.83$ rad, $\Delta\phi_4 = 0.98$ rad, $w_{GM1} = 0.52$, $w_{VL1} = 0.13$, $w_{SO1} = 0.34$, $w_{BF1} = 0.14$, $w_{GA1} = 0.34$, $w_{GM2} = 0.22$, $w_{VL2} = 0.16$, $w_{SO2} = 0.11$, $w_{BF2} = 0.08$, $w_{GA2} = 0.04$, $w_{IP3} = 0.20$, $w_{TA3} = 0.11$, $w_{BF3} = 0.05$, $w_{IP4} = 0.20$, and $w_{TA4} = 0.03$, where we set $\phi = 0$ rad at foot contact. The other weighting coefficients were set to zero. We determined the gain parameter, which controls the interlimb coordination pattern, by $K_\phi = 5.0$ to obtain a high performance of the obstacle avoidance (see Section 5.2).

We determined the parameter for phase resetting by $\phi^{\text{Contact}} = 0.25$ rad, so that the phase value just before resetting by delayed tactile sensory information is identical to the parameter during steady walking, that is, the steady locomotion with phase resetting is the same as without phase resetting.

Regarding the posture control, we determined $\hat{h}^{\text{Hip}} = 0.051$ m and $\hat{v}^{\text{COM}} = 0.35$ m/s from the results of simulation with empirical kinematic data. The gain parameters were determined through modulation of the second step of parameter determination as follows: $K_{VL}^{\text{Hgt}} = 20$, $K_{TA}^{\text{Hgt}} = -20$, $K_{SO}^{\text{Hgt}} = 20$, $D_{VL}^{\text{Hgt}} = 0.01$, $D_{TA}^{\text{Hgt}} = -0.01$, $D_{SO}^{\text{Hgt}} = 0.01$, $K_{IP}^{\text{COM}} = -1.4$, $K_{GM}^{\text{COM}} = 1.4$, $K_{TA}^{\text{COM}} = -0.7$, and $K_{SO}^{\text{COM}} = 0.7$.

A.2 Parameters for obstacle avoidance

We determined the parameters for obstacle avoidance similarly to those for the movement control of periodic limb movements described in Appendix A.1. We conducted the computer simulation using PD feedback control based on the empirical kinematic data of obstacle avoidance. Based on the PCA for the simulated muscle activation patterns, we determined the parameters for the additional rectangular pulse ($P_{\text{Lead,Trail}}$) as follows: $\phi_{\text{Lead}}^{\text{Start}} = 3.26$ rad, $\phi_{\text{Trail}}^{\text{Start}} = 3.26$ rad, $\Delta\phi_{\text{Lead}} = 1.76$ rad, $\Delta\phi_{\text{Trail}} = 0.25$ rad, $w_{IP,\text{Lead}}^{\text{Ipsi}} = 0.98$, $w_{TA,\text{Lead}}^{\text{Ipsi}} = 0.13$, $w_{GM,\text{Lead}}^{\text{Contra}} = 0.44$, $w_{VL,\text{Lead}}^{\text{Contra}} = 1.00$, $w_{SO,\text{Lead}}^{\text{Contra}} = 0.13$, $w_{GM,\text{Trail}}^{\text{Ipsi}} = 0.26$, $w_{TA,\text{Trail}}^{\text{Ipsi}} = 0.88$, $w_{GA,\text{Trail}}^{\text{Ipsi}} = 0.50$, $w_{VL,\text{Trail}}^{\text{Contra}} = 0.13$, and $w_{SO,\text{Trail}}^{\text{Contra}} = 0.13$. The other weighting coefficients were set to zero.

Acknowledgements This paper is supported in part by a Grant-in-Aid for Scientific Research (B) No. 23360111 and a Grant-in-Aid for Creative Scientific Research No. 19GS0208 from the Ministry of Education, Culture, Sports, Science, and Technology of Japan.

References

- Akay *et al.* 2006. Akay, T., Acharya, H.J., Fouad, K., and Pearson, K.G. (2006) *Behavioral and electromyographic characterization of mice lacking EphA4 receptors*, J. Neurophysiol., 96:642–651.
- Aoi *et al.* 2010. Aoi, S., Ogihara, N., Funato, T., Sugimoto, Y., and Tsuchiya, K. (2010) *Evaluating functional roles of phase resetting in generation of adaptive human bipedal walking with a physiologically based model of the spinal pattern generator*, Biol. Cybern., 102(5):373–387.
- Aoi *et al.* 2012. Aoi, S., Ogihara, N., Funato, T., and Tsuchiya, K. (2012) *Sensory regulation of stance-to-swing transition in generation of adaptive human walking: A simulation study*, Robot. Auton. Syst., 60(5):685–691.
- Asai *et al.* 2009. Asai, Y., Tasaka, Y., Nomura, K., Nomura, T., Casadio, M., and Morasso, P. (2009) *A model of postural control in quiet standing: robust compensation of delay-induced instability using intermittent activation of feedback control*, PLoS One, 4(7):e6169.
- Austin *et al.* 1999. Austin, G.P., Garrett, G.E., and Bohannon, R.W. (1999) *Kinematic analysis of obstacle clearance during locomotion*, Gait Posture, 10:109–120.
- Bosco and Poppele 2001. Bosco, G. and Poppele, R.E. (2001) *Proprioception from a spinocerebellar perspective*, Physiol. Rev., 81:539–568.
- Burke *et al.* 2001. Burke, R.E., Degtyarenko, A.M., and Simon, E.S. (2001) *Patterns of locomotor drive to motoneurons and last-order interneurons: Clues to the structure of the CPG*, J. Neurophysiol., 86:447–462.
- Burkholder and Nichols 2004. Burkholder, T.J. and Nichols, T.R. (2004) *Three-dimensional model of the feline hindlimb*, J. Morph., 261(1):118–129.
- Cappellini *et al.* 2006. Cappellini, G., Ivanenko, Y.P., Poppele, R.E., and Lacquaniti, F. (2006) *Motor patterns in human walking and running*, J. Neurophysiol., 95:3426–3437.
- Casabona *et al.* 2003. Casabona, A., Valle, M.S., Bosco, G., Garifoli, A., Lombardo, S.A., and Perciavalle, V. (2003) *Anisotropic representation of forelimb position in the cerebellar cortex and nucleus interpositus of the rat*, Brain Res., 972:127–136.
- Casabona *et al.* 2004. Casabona, A., Valle, M.S., Bosco, G., and Perciavalle, V. (2004) *Cerebellar encoding of limb position*, Cerebellum, 3:172–177.
- Chonga *et al.* 2009. Chonga, R.K.Y., Chastan, N., Welter, M.L., and Do, M.C. (2009) *Age-related changes in the center of mass velocity control during walking*, Neurosci. Lett., 458:23–27.
- Chou and Draganich 1998. Chou, L.S. and Draganich, L.F. (1998) *Increasing obstacle height and decreasing toe-obstacle distance affect the joint moments of the stance limb differently when stepping over an obstacle*, Gait Posture, 8:186–204.
- Conway *et al.* 1987. Conway, B.A., Hultborn, H., and Kiehn, O. (1987) *Proprioceptive input resets central locomotor rhythm in the spinal cat*, Exp. Brain Res., 68:643–656.
- d’Avella and Bizzi 2005. d’Avella, A. and Bizzi, E. (2005) *Shared and specific muscle synergies in natural motor behaviors*, Proc. Natl. Acad. Sci. USA, 102(8):3076–3081.

-
- d'Avella *et al.* 2003. d'Avella, A., Saltiel, P., and Bizzi, E. (2003) *Combinations of muscle synergies in the construction of a natural motor behavior*, Nat. Neurosci., 6:300–308.
- Dominici *et al.* 2011. Dominici, N., Ivanenko, Y.P., Cappellini, G., d'Avella, A., Mondì, V., Cicchese, M., Fabiano, A., Silei, T., Di Paolo, A., Giannini, C., Poppele, R.E., and Lacquaniti, F. (2011) *Locomotor primitives in newborn babies and their development*, Science, 334(6058):997–999.
- Drew *et al.* 2008. Drew, T., Kalaska, J., and Krouchev, N. (2008) *Muscle synergies during locomotion in the cat: a model for motor cortex control*, J. Physiol., 586(5):1239–1245.
- Duysens and Pearson 1980. Duysens, J. and Pearson, K.G. (1980) *Inhibition of flexor burst generation by loading ankle extensor muscles in walking cats*, Brain Res., 187:321–332.
- Duysens 1977. Duysens, J. (1977) *Fluctuations in sensitivity to rhythm resetting effects during the cat's step cycle*, Brain Res., 133(1):190–195.
- Duysens *et al.* 2000. Duysens, J., Clarac, F., and Cruse, H. (2000) *Load-regulating mechanisms in gait and posture: Comparative aspects*, Physiol. Rev., 80:83–133.
- Ekeberg and Pearson 2005. Ekeberg, Ö. and Pearson, K. (2005) *Computer simulation of stepping in the hind legs of the cat: An examination of mechanisms regulating the stance-to-swing transition*, J. Neurophysiol., 94:4256–4268.
- Forssberg and Grillner 1973. Forssberg, H. and Grillner, S. (1973) *The locomotion of the acute spinal cat injected with clonidine i.v.*, Brain Res., 50:184–186.
- Grillner 1975. Grillner, S. (1975) *Locomotion in vertebrates: central mechanisms and reflex interaction*, Physiol. Rev., 55(2):247–304.
- Gruner *et al.* 1980. Gruner, J.A., Altman, J., and Spivack, N. (1980) *Effects of arrested cerebellar development on locomotion in the rat cinematographic and electromyographic analysis*, Exp. Brain Res., 40:361–373.
- Guertin *et al.* 1995. Guertin, P., Angel, M.J., Perreault, M.-C., and McCrea, D.A. (1995) *Ankle extensor group I afferents excite extensors throughout the hindlimb during fictive locomotion in the cat*, J. Physiol., 487(1):197–209.
- Guertin 2009. Guertin, P.A. (2009) *The mammalian central pattern generator for locomotion*, Brain Res. Rev., 62:45–56.
- Ichise *et al.* 2000. Ichise, T., Kano, M., Hashimoto, K., Yanagihara, D., Nakao, K., Shigemoto, R., Katsuki, M., and Aiba, A. (2000) *mGluR1 in cerebellar Purkinje cells essential for long-term depression, synapse elimination, and motor coordination*, Science, 288(5472):1832–1835.
- Ivanenko *et al.* 2004. Ivanenko, Y.P., Poppele, R.E., and Lacquaniti, F. (2004) *Five basic muscle activation patterns account for muscle activity during human locomotion*, J. Physiol., 556:267–282.
- Ivanenko *et al.* 2005. Ivanenko, Y.P., Cappellini, G., Dominici, N., Poppele, R.E., and Lacquaniti, F. (2005) *Coordination of locomotion with voluntary movements in humans*, J. Neurosci., 25(31):7238–7253.
- Ivanenko *et al.* 2006. Ivanenko, Y.P., Poppele, R.E., and Lacquaniti, F. (2006) *Motor control programs and walking*, Neuroscientist, 12(4):339–348.
- Ivashko *et al.* 2003. Ivashko, D.G., Prilutsky, B.I., Markin, S.N., Chapin, J.K., and Rybak, I.A. (2003) *Modeling the spinal cord neural circuitry controlling cat hindlimb movement during locomotion*, Neurocomputing, 52-54:621–629.
- Jo and Massaquoi 2007. Jo, S. and Massaquoi, S.G. (2007) *A model of cerebrocerebello-spinomuscular interaction in the sagittal control of human walking*, Biol. Cybern., 96:279–307.

-
- Jo 2008. Jo, S. (2008) *Hypothetical neural control of human bipedal walking with voluntary modulation*, Med. Bio. Eng. Comput., 46:179–193.
- Johnson *et al.* 2008. Johnson, W.L., Jindrich, D.L., Roy, R.R., and Edgerton, V.R. (2008) *A three-dimensional model of the rat hindlimb: Musculoskeletal geometry and muscle moment arms*, J. Biomech., 41(3):610–619.
- Kondo *et al.* 2010. Kondo, T., Aoi, S., Yanagihara, D., Aoki, S., Yamaura, H., Ogihara, N., Ichikawa, A., and Tsuchiya, K. (2010) *Development of a musculoskeletal model of the hind legs of the rat based on anatomical data and generation of locomotion based on kinematic data*, Proc. SICE Ann. Conf., pp. 2308–2310.
- Lafreniere-Roula and McCrea 2005. Lafreniere-Roula, M. and McCrea, D.A. (2005) *Deletions of rhythmic motoneuron activity during fictive locomotion and scratch provide clues to the organization of the mammalian central pattern generator*, J. Neurophysiol., 94:1120–1132.
- Latash 2008. Latash, M.L. (2008) *Synergy*, Oxford University Press.
- Lockhart and Ting 2007. Lockhart, D.B. and Ting, L.H. (2007) *Optimal sensorimotor transformations for balance*, Nat. Neurosci., 10(10):1329–1336.
- McCrea and Rybak 2008. McCrea, D.A. and Rybak, I.A. (2008) *Organization of mammalian locomotor rhythm and pattern generation*, Brain Res. Rev., 57:134–146.
- Markin *et al.* 2010. Markin, S.N., Klishko, A.N., Shevtsova, N.A., Lemay, M.A., Prilutsky, B.I., and Rybak, I.A. (2010) *Afferent control of locomotor CPG: insights from a simple neuromechanical model*, Ann. N.Y. Acad. Sci., 1198:21–34.
- Masani *et al.* 2003. Masani, K., Popovic, M.R., Nakazawa, K., Kouzaki, M., and Nozaki, D. (2003) *Importance of body sway velocity information in controlling ankle extensor activities during quiet stance*, J. Neurophysiol., 90:3774–3782.
- Masani *et al.* 2006. Masani, K., Vette, A.H., and Popovic, M.R. (2006) *Controlling balance during quiet standing: Proportional and derivative controller generates preceding motor command to bodysway position observed in experiments*, Gait Posture, 23(2):164–172.
- Maurer and Peterka 2005. Maurer, C. and Peterka, R.J. (2005) *A new interpretation of spontaneous sway measures based on a simple model of human postural control*, J. Neurophysiol., 93:189–200.
- Muramatsu *et al.* 2009. Muramatsu, H., Suzuki, K., Sasaki, T., Matsumoto, M., Sakuma, J., Oinuma, M., Itakura, T., and Kodama, N. (2009) *Evoked potentials elicited on the cerebellar cortex by electrical stimulation of the rat spinocerebellar tract*, Surg. Neurol., 72:395–400.
- Orlovsky *et al.* 1999. Orlovsky, G.N., Deliagina, T., and Grillner, S. (1999) *Neuronal control of locomotion: from mollusc to man*, Oxford University Press.
- Patla and Greig 2006. Patla, A.E. and Greig, M. (2006) *Any way you look at it, successful obstacle negotiation needs visually guided on-line foot placement regulation during the approach phase*, Neurosci. Lett., 397:110–114.
- Pearson *et al.* 2005. Pearson, K.G., Acharya, H., and Fouad, K. (2005) *A new electrode configuration for recording electromyographic activity in behaving mice*, J. Neurosci. Meth., 148:36–42.
- Peterka 2000. Peterka, R.J. (2000) *Postural control model interpretation of stabilogram diffusion analysis*, Biol. Cybern., 82:335–343.
- Poppele *et al.* 2002. Poppele, R.E, Bosco, G., and Rankin, A.M. (2002) *Independent representations of limb axis length and orientation in spinocerebellar response components*, J. Neurophysiol., 87:409–422.
- Poppele and Bosco 2003. Poppele, R.E. and Bosco, G. (2003) *Sophisticated spinal contributions to motor control*, Trends. Neurosci., 26:269–276.

-
- Rybak *et al.* 2006a. Rybak, I.A., Shevtsova, N.A., Lafreniere-Roula, M., and McCrea, D.A. (2006) *Modelling spinal circuitry involved in locomotor pattern generation: insights from deletions during fictive locomotion*, *J. Physiol.*, 577(2):617–639.
- Rybak *et al.* 2006b. Rybak, I.A., Stecina, K., Shevtsova, N.A., and McCrea, D.A. (2006) *Modelling spinal circuitry involved in locomotor pattern generation: insights from the effects of afferent stimulation*, *J. Physiol.*, 577(2):641–658.
- Sato *et al.* 2012. Sato, Y., Aoki, S., and Yanagihara, D. (2012) *Gait modification during approach phase when stepping over an obstacle in rats*, *Neurosci. Res.*, 72(3):263–269.
- Schomburg *et al.* 1998. Schomburg, E.D., Petersen, N., Barajon, I., and Hultborn, H. (1998) *Flexor reflex afferents reset the step cycle during fictive locomotion in the cat*, *Exp. Brain Res.*, 122(3):339–350.
- Shik and Orlovsky 1976. Shik, M.L. and Orlovsky, G.N. (1976) *Neurophysiology of locomotor automatism*, *Physiol. Rev.*, 56(3):465–501.
- Taga *et al.* 1991. Taga, G., Yamaguchi, Y., and Shimizu, H. (1991) *Self-organized control of bipedal locomotion by neural oscillators in unpredictable environment*, *Biol. Cybern.*, 65:147–159.
- Taga 1995. Taga, G. (1995) *A model of the neuro-musculo-skeletal system for human locomotion I. Emergence of basic gait*, *Biol. Cybern.*, 73:97–111.
- Taga 1998. Taga, G. (1998) *A model of the neuro-musculo-skeletal system for anticipatory adjustment of human locomotion during obstacle avoidance*, *Biol. Cybern.*, 78:9–17.
- Ting and Macpherson 2005. Ting, L.H. and Macpherson, J.M. (2005) *A limited set of muscle synergies for force control during a postural task*, *J. Neurophysiol.*, 93:609–613.
- Todorov and Jordan 2002. Todorov, E. and Jordan, M.I. (2002) *Optimal feedback control as a theory of motor coordination*, *Nat. Neurosci.*, 5:1226–1235.
- Welch and Ting 2008. Welch, T.D.J. and Ting, L.H. (2008) *A feedback model reproduces muscle activity during human postural responses to support-surface translations*, *J. Neurophysiol.*, 99:1032–1038.
- Yakovenko *et al.* 2004. Yakovenko, S., Gritsenko, V., and Prochazka, A. (2004) *Contribution of stretch reflexes to locomotor control: A modeling study*, *Biol. Cybern.*, 90:146–155.
- Yamasaki *et al.* 2003a. Yamasaki, T., Nomura, T., and Sato, S. (2003) *Phase reset and dynamic stability during human gait*, *BioSystems*, 71:221–232.
- Yamasaki *et al.* 2003b. Yamasaki, T., Nomura, T., and Sato, S. (2003) *Possible functional roles of phase resetting during walking*, *Biol. Cybern.*, 88:468–496.
- Yanagihara *et al.* 1993. Yanagihara, D., Udo, M., Kondo, I., and Yoshida, T. (1993) *A new learning paradigm: adaptive changes in interlimb coordination during perturbed locomotion in decerebrate cats*, *Neurosci. Res.*, 18(3):241–244.
- Yanagihara and Kondo 1996. Yanagihara, D. and Kondo, I. (1996) *Nitric oxide plays a key role in adaptive control of locomotion in cat*, *Proc. Natl. Acad. Sci. USA*, 93:13292–13297.